Article Type: Original Article

Title: New insights into the lymphovascular microanatomy of the colon and the risk of metastases in pT1 colorectal cancer using quantitative methods and 3 dimensional digital reconstruction

Running title: Vascular microanatomy

Keywords: Colorectal cancer, microvessel anatomy, submucosal plexus, CD31.

Authors

Peter J Brown[1, 2], Eu-Wing Toh[1, 2, 3], Katherine JE Smith[1, 2, 3, 4], Pamela Jones[5], Darren Treanor[1,2], Derek Magee[6], Dermot Burke[2, 3], Phil Quirke[1, 2].

Affiliations

1. Pathology and Tumour Biology, Leeds Institute of Cancer and Pathology, Level 4 Wellcome Trust Brenner Building, St James's University Hospital, Leeds LS9 7TF, UK

2. Leeds Teaching Hospitals Trust, Leeds, UK, LS9 7TF

3. Translational Anaesthetic and Surgical Science, Leeds Institute of Biological and Clinical Sciences, Clinical Sciences Building, St James's University Hospital, Leeds LS9 7TF, UK

This article has been accepted for publication and undergone full peer review but has not been through the copyediting, typesetting, pagination and proofreading process which may lead to differences between this version and the Version of Record. Please cite this article as an 'Accepted Article', doi: 10.1111/his.12639

4. Nottingham University Hospitals, Nottingham, NG7 2UH.

5. Section of Molecular Gastroenterology, Leeds Institute of Biological and Clinical Sciences, Level 9 Wellcome Trust Brenner Building, St James's University Hospital, Leeds LS9 7TF, UK

6. School of Computing, University of Leeds, Leeds LS2 9JT, UK

Author responsible for correspondence

Professor Phil Quirke,

Pathology and Tumour Biology,

Leeds Institute of Molecular Medicine,

Level 4 Wellcome Trust Brenner Building,

St James's University Hospital,

Leeds,

LS9 7TF,

UK

Tel: 0113 3438407 Fax: 0113 3438431

Email p.quirke@leeds.ac.uk

No authors are aware of any conflicts of interest to declare.

Abstract

Introduction: UK Faecal Occult Blood Testing screening has tripled the proportion of pT1 colorectal cancers. Risk of metastasis is predicted by depth of invasion suggesting access to

deep lymphovascular vessels is important. We quantified the distribution and size of the submucosal vasculature and generated a novel 3D model to validate the findings.

Method: Thirty samples of normal large bowel wall were immunostained with CD31 a vascular endothelium marker to identify blood vessels which were quantified and digitally analysed for their number, circumference, area and diameter in the deep *mucosa* and submucosa (sm1,2 and 3). The model required serial sections, a double immunostain (using CD31 and D2-40) and 3D reconstruction.

Results: Significant differences were shown between submucosal layers for the number, circumference and area of vessels ($p<0.001$). Bloods vessels were most numerous in the mucosa (11.79vessels/0.2mm^2) but smallest (median area 247μm^2(IQR:162-373μm^2)) compared to sm2 where they were fewer (6.92vessels/0.2mm^2) but considerably larger (2086μm^2(IQR:1007-4784μm^2)). The 3D model generated novel observations on lymphovascular structures.

Discussion: The number and size of blood vessels does not increase with depth of submucosa as hypothesised. The distribution of vessels suggests that we should investigate the area or volume of submucosal invasion rather than the depth.

INTRODUCTION

Colorectal cancer (CRC) is the third most common cancer in the UK(1). To detect tumours at earlier stages and so reduce the morbidity and mortality of CRC the national faecal occult blood test (FOBT) screening programme was initiated in the UK; many other western countries have since adopted similar schemes(1-3).

Since the introduction of screening in the UK in 2006, the proportion of Dukes' stage A cancers has risen significantly(4-7). Such early stage cancers have a low risk of both lymph node metastasis (LNM) and distant metastatic spread(6). Early tumours requiring a major resection due to a high risk of metastatic spread are currently identified based on histopathological risk factors, which are: poor differentiation, depth and width of tumour invasion and lymphatic or vascular invasion(4-8). Of these, depth of tumour invasion is widely used as a predictor of spread when poor differentiation, lymphatic or vascular invasion are absent.

Multiple methods of quantifying the depth of tumour invasion into the submucosa have been described e.g Haggitt *et al*(5) for polypoid lesions and Kikuchi *et al*(7) for sessile lesions. Haggitt showed that invasion beyond the polyp stalk into the submucosa is an adverse prognostic factor in terms of local disease spread and mortality(5). Sakatani *et al*(9) first described the division of submucosal invasion into 3 levels and later on, Kikuchi *et al*(7) demonstrated the risk of LNM varied from 2% in the most superficial layer to 23% in the deepest. Meanwhile other studies have given absolute values of submucosal invasion, such as 1000µm(8, 10), 1800 µm(11) or 2000µm(8, 12, 13) beyond which the risk of LNM significantly increases. In Japan these measurements are then used to guide treatment with surgical resections, instead of endoscopic resections, being offered when tumours extend beyond 1000µm(14).

Our understanding of why tumours invading deeply into the submucosa have a significantly higher risk of LNM is very limited. Our previous study of lymphatic vessels has helped understand the anatomical basis for the increased risk of metastasis associated with the

area and width of invasion(15). Here we sought to further investigate this issue by studying whether the number or architecture of blood vessels in the submucosa can provide further insight into the mechanisms of spread in pT1 cancers. Additionally, a 3-dimensional (3D) model of the lymphatic and vascular structures was generated using 3D digital pathology(16) to qualitatively (visually) validate the result observed in the quantitative 2D analysis.

MATERIALS AND METHODS

Thirty samples of normal colorectal tissue were prospectively collected with informed consent (Local Ethical Approval 08/H1313/84) from patients undergoing elective surgery for CRC at Leeds Teaching Hospitals, Leeds, UK. Patients with multiple tumours or those who had emergency resections were excluded from the study. Normal tissues were defined as located a minimum of 10cm from the tumour border with normal morphology as assessed by a gastrointestinal pathologist (PQ). The same samples were previously studied for the presence of lymphatic vessels(15). Samples were initially fixed in formalin and embedded in paraffin. For quantitation, 5µm sections were used and every tenth section mounted on slides (Superfrost plus+ coated slides, SolMedia Laboratory Supplies, Romford, UK). For the 3D model, 72 sequential 5µm sections were used.

Tissues were stained using immunohistochemistry for accurate identification of vessels: CD31 (Dako, IR610, Ely, UK) for vascular endothelial cells and D2-40 (Dako, M3619, Ely, UK) for lymphatic endothelial cells. A combination of both antibodies was performed as a double stain for the 3D model, Figure 1.

In brief, paraffin sections were dewaxed, rehydrated and antigen retrieval performed using 1% Antigen Unmasking Solution and a pressure cooker. A hydrogen peroxidase block (Dako Mouse EnVision™ kit, Dako, Ely, UK) was applied to slides mounted in the Sequenza apparatus, for CD31 and D2-40, and a humidified flatbed chamber for the double stain. Casein solution was added, at 10% concentration, then primary antibodies applied and incubated; overnight for CD31, 45 minutes at 37°C for D2-40 and the double stain. The secondary antibody was applied, following manufacturers' guidelines incubated for 30 minutes and then developed with diaminobenzidine tetrahydrochlorine in a humidified incubator. The double stain was additionally developed over a 20 minute incubation with Fast Red. Counterstaining, dehydration and mounting, using DePex was then performed. Stained sections were scanned using the high-resolution Aperio ScanScope® (Vista, CA, USA) at 400X magnification and digitalised images uploaded onto a PC.

Vessel morphometry was assessed on digitalised slides, using Aperio ImageScope® software; by an identical method to that previously described(15). Boxes of fixed area (0.20 mm^2) were placed at random in the deep mucosa, abutting the *muscularis mucosa* and columns of three additional boxes then placed below in thirds of the submucosa, sm1, sm2 and sm3; figure 2A. Within each box vessels were identified, counted and manually annotated on the software, which then calculated luminal circumference, area and measured the diameter of vessels (Figure 2B).

Immunohistochemistry with anti-CD31 resulted in the staining of blood vessels and some lymphatic vessels (due to cross-reactivity between antigens). These were quantified using D2-40 and double-staining techniques on serial sections. Further the identification of blood vessels relied on the presence of immunostaining and the fulfilment of defined criteria to

ensure the exclusion of lymphatic vessels. Where ambiguous, any immunostaining of endothelial cells or cell clusters was only deemed a blood vessel if; it was clearly separate from adjacent micro-vessels and other connective tissue elements, it had a lumen either containing red blood corpuscles or in their absence, a regular circumference.

The method for statistical analysis also followed those previously used(15). A mean value was calculated for vessel characteristics within each box and then within each layer (mucosal, sm1, sm2 and sm3) for each patient, calculated from the 12 boxes per layer assessed for each patient. Running mean calculations showed the assessment of 12 boxes per layer per patient reduced variation below 5% between individual measurements providing a reliable and accurate value. Quantitative data for vessel morphometry were analysed using Pearson's Chi-Squared, Mann-Whitney U and Kruskal-Wallis tests using Statistical Package for the Social Sciences (SPSS, v16.0 IBM, Chicago, IL, USA). The threshold for statistical significance was considered $p<0.05$.

3D Model

For the 3D model, digitised images of the double immunostained slides were uploaded onto a PC. An identical area of full thickness bowel wall was isolated in each image on Aperio ImageScope® allowing visualisation of the same region in each slide. Blood and lymphatic vessels were identified and annotated, as were the *muscularis propria, muscularis mucosa* and mucosal lymphoid follicles to act as anatomical landmarks. Software developed in partnership between the School of Computing and the Section of Pathology and Tumour Biology at the University of Leeds was used to combine the annotations from each digital slide, as described by Roberts *et al*(16). This generated a virtual 3D model that could be

manipulated to be viewed in different planes and orientations and have its constituent objects, such as the *muscularis propria* removed for easier visualisation of the vessel architecture.

RESULTS

Thirty tissue samples were collected from 26 patients, 4 of whom had 2 samples analysed from different locations within the large intestine. Table 1 shows demographic information in more detail. Analysis of pre-operative treatment showed no significant difference in vessel characteristics, p=0.256.

The immunohistochemistry protocol for CD31 produced consistent and precise identification of blood vessels, and has been previously reported(17-22). The extent of CD31 cross-reactivity and subsequent staining of lymphatic vessels was quantified on serially sectioned slides using an additional D2-40 marker. These data were shown to be insignificant when compared to the total number of vessels stained (p= 1.00, Mann-Whitney U test). Investigator dependent error was scrutinised through a second blinded investigator (KS) independently scoring a randomly selected set of 12 columns for one patient. Analysis of reproducibility showed insignificant inter-observer variability for all variables ($p>0.05$; p=0.886 for vessel number ranging to p=0.686 for vessel circumference: Mann-Whitney U test).

Data were analysed to assess differences in blood vessel number and characteristics between all layers as well as mucosal and submucosal (sm1, sm2 and sm3). Differences between all the layers (mucosa v sm1 v sm2 v sm3) were significantly different for all four variables, $p<0.001$, Mann-Whitney U test (Table 2).

The number and median circumference of blood vessels varied significantly across layers ($p<0.001$, Kruskal Wallis Test). Within the submucosa there were significantly more vessels in sm1 [11.4 vessels per 0.2mm^2 (IQR, 9.2- 14.8 vessels per 0.2mm^2)] compared to deeper layers, sm2 and sm3 ($P < 0.001$, Mann-Whitney U test). As shown in Table 2A, vessels in sm2 had the largest median circumference [134.4 µm per vessel (IQR, 85.2-156.1 µm per vessel)] and largest median area [2085.6 µm^2 per vessel (IQR, 1007.0-4783.5 µm^2 per vessel)]. Blood vessels in the mucosa had the smallest median circumference [61.9 µm per vessel (IQR, 53.9-72.2 µm per vessel)] and smallest median area [247.1 µm^2 per vessel (IQR, 162.0-373.2 µm^2 per vessel)]. Table 2B shows that statistical significance was achieved across this and a range of other comparisons between layers. Comparing regions of the submucosa, differences in the median vessel circumference between sm1 and sm2 were not statistically significant. However, the median vessel circumference and median vessel area in sm3 were both significantly smaller than the median vessel circumference and area of vessels in sm1 and sm2.

3D data and image

The 3D model, figure 3, demonstrates small blood vessels (red) throughout the mucosa with lymphatics (yellow) confined to the base of the mucosa (dark blue), where they interweave with the *muscularis mucosae* (bright blue). Larger collections of lymphatics are lying underneath lympho-glandular complexes (purple). There are two major layers of blood vessels within the submucosa and a major channel of vessels and lymphatics as they cluster to leave the submucosa and pass through the *muscularis propria*. The two layers of the *muscularis propria* were hypovascular with some vessels lying with the myenteric plexus

between muscular layers. There was a further rich plexus of vessels and lymphatics seen in a layer just outside the *muscularis propria*.

DISCUSSION

The physical number and size of blood vessels in the mucosa and sm1-3 varies significantly, showing a similar pattern of distribution in the submucosa to lymphatic studies(15). The mucosa contained small blood vessels spread throughout its whole thickness; as opposed to the lymphatic system, that was shown to be confined to base of the mucosa and formed prominent lymphatic complexes at the base of lymphoid follicles.

Vessel number and size were not found to increase in deeper submucosal layers despite penetration by the tumour to this region being associated with a higher risk of lymph node metastasis(5, 7, 10-13, 23). Our quantitative analysis of the micro-anatomical distribution of blood and lymphatic vessels of the colon and rectum does not explain the simple model of the increased risk of tumour spread associated with increasing depth of penetration.

Intuitively there should be fewer, larger vessels in deeper layers of the submucosa because small capillaries unite to form small veins as they pass into deeper tissues. A similar pattern is expected with the lymphatic vessels and the arteries. However, the rate of change between layers in the number of vessels, their median circumference and area between the 4 layers, as shown in Figure 4, does not correlate with the rate of increase of metastasis. This demonstrates that depth of invasion alone to sm3 is not the only factor affecting the metastatic risk.

The risk of vessel invasion is related not only to each layer, but also the sum of each of the preceding layers. Therefore, when comparing two pT1 colorectal cancers with different depths of invasion (sm1 cancer vs sm3 cancer), the sm3 cancer would have traversed sm1 and sm2 layers. This sm3 cancer will then have an increased area of submucosal invasion leading to an increased likelihood of the cancer coming into contact with and invading vessels compared to a sm1 cancer. As a measure of the potential blood vessels encountered by tumours we assessed the accumulated circumference and area; (calculated from the sum of the median values obtained for preceding layers) this increases between submucosal layers, Figure 4. However, the increase is not at the reported rate of LNM. Superficial sm1 or sm2 tumours with a broad invasive front may pose a higher risk of LNM than some "narrowly invasive" sm3 tumours given the low density of lymphatic and blood vessels in sm3 and the higher density of lymphatic vessels in sm1 and blood vessels in sm1 and sm2(15). Similarly, the presence of tumour budding will increase the area and volume of tumour invasion; this might account for the associated increase in the rate of LNM and worse outcomes in early CRCs where tumour budding is present(24).

We found no difference in the properties of blood vessels based on preoperative treatment; however, samples taken were out of the field of radiation and this study was not designed to look at the effects of preoperative treatment. Similarly, we found no differences between blood vessels in the colon or rectum suggesting that any reported differences in the frequency of LNM in these tumours, if real, must be caused by differences in the biology of these tumours.

The observation of larger vessels within sm2 as supported by the 3D as it confirmed previous reports of a sub-mucosal plexus existing around the circumference and along the length of the colon(25, 26). Arteries pass between the longitudinal muscle layer within the *muscularis propria* and then puncture through the circular muscle to the submucosa(25, 26). Within the submucosa vessels form a plexus to perfuse surrounding tissues and allow absorption of fluid from the mucosal surface. The vessel morphometry data presented here suggest that the submucosal plexus is located within the middle third of the submucosa. This plexus has been further divided into a 'macromesh and micromesh' accounting for the large and small networks of blood vessels(25). The 3D model supports this theory by showing a plexus of small blood vessels just below the *muscularis mucosae*, in addition to the plexus in sm2 containing larger vessels. The presence of two plexuses could be explained by separating the arteries and veins, a limitation of our study; histological separation of blood vessels to ascertain the separate blood supply and drainage could enable this.

The number or size of lymphatic(15) and now blood vessels, do not increase in the deepest layer of the submucosa. Therefore, the observed risk of lymph node metastasis increasing with depth of invasion into the submucosa does not appear to be explained by the size or number of blood or lymphatic vessels within sm3. In the future we need to robustly investigate the width of invasion and the tumour area and volume of submucosal invasion to assess their benefit in predicting the risk of LNM in both the symptomatic and screened populations. The 3D model confirmed these findings and showed: 1)at the base of each lymphoid follicle there is a lymphatic complex possibly increasing the risk of lymphatic

metastasis when their number is increased, 2) the convergence of the arteries, veins and lymphatics to penetrate the muscularios propria forms a rich lymphovascular complex and early tumours overlying these areas may have an increased risk of metastases and 3) there is a further lymphovascular complex on the external surface of the *muscularis propria* that may account for the prognostic importance of depth of spread in colorectal adenocarcinomas. This is currently under further study.

Funding Yorkshire Cancer Research and National Health Service (England) Bowel Cancer Screening Programme

PB was supported by Yorkshire Cancer Research, the Pathological Society of Great Britain and Ireland and the Association of Clinical Pathologists. KS, ET and PQ were supported by Yorkshire Cancer Research and the National Health Service (England) Bowel Cancer Screening Programme. DT by the National Institute of Health Research.

Author Contributions

Peter Brown	Data collection, analysis and interpretation. Writing of paper and final approval.
Eu-Wing Toh	Data collection, analysis and interpretation. Writing of paper and final approval.
Katherine Smith	Project conception, data collection, analysis and interpretation. Writing of paper and final approval.

Pamela Jones	Project conception, data interpretation and final approval.
Darren Treanor	Project conception 3D component and final approval.
Derek Magee	Software development, 3D support and final approval.
Dermot Burke	Project conception, data collection, analysis and interpretation. Writing of paper and final approval.
Phil Quirke	Project conception, data collection, analysis and interpretation. Writing of paper and final approval.

References

1. ONS. Cancer Registrations in England 2010. Number of newly diagnosed cases of cancer in males and females, England, 2010: most common sites. Pub. 2012. Office of National Statistics.
2. EU. Report from the commision to the council, the European parliment, the European ecconomic and social committee of the regions. Implementation of the Council Recommendation of 2 December 2003 on cancer screening (2003/878/EC). Commission of the European Commiunities. Brussels, 2008.
3. Segnan N, Patnick, J, von Karsa, L. European guidelines for quality assurance in colorectal cancer screening and diagnosis - First edition. Eurpoean Commision, International Agency on Research in Cancer2010.
4. Greene FL. AJCC cancer staging handbook : from the AJCC cancer staging manual. American Joint Committee on Cancer, American Cancer Society. 6th ed. New York: Springer; 2002.
5. Haggitt RC, Glotzbach RE, Soffer EE, Wruble LD. Prognostic factors in colorectal carcinomas arising in adenomas: implications for lesions removed by endoscopic polypectomy. Gastroenterology. 1985;89:328-36.
6. Hamilton SR, Aaltonen LA, International Agency for Research on Cancer., World Health Organization. Pathology and genetics of tumours of the digestive system. Lyon: IARC Press; 2000.
7. Kikuchi R, Takano M, Takagi K, et al. Management of early invasive colorectal cancer. Risk of recurrence and clinical guidelines. Dis Colon Rectum. 1995;38:1286-95.
8. Ueno H, Mochizuki H, Hashiguchi Y, et al. Risk factors for an adverse outcome in early invasive colorectal carcinoma. Gastroenterology. 2004;127:385-94.
9. Sakatani A, Koizumi K, Maruyama M. Diagnosis of sm cancer of the large intestine - with special reference to its x-ray diagnosis. Stomach and Intestine. 1991;26:726 - 35.
10. Tateishi Y, Nakanishi Y, Taniguchi H, Shimoda T, Umemura S. Pathological prognostic factors predicting lymph node metastasis in submucosal invasive (T1) colorectal carcinoma. Mod Pathol. 2010;23(8):1068-72.
11. Nakadoi K, Tanaka S, Kanao H, et al. Management of T1 colorectal carcinoma with special reference to criteria for curative endoscopic resection. J Gastroenterol Hepatol. 2012;27(6):1057-62.

12. Sakuragi M, Togashi K, Konishi F, et al. Predictive factors for lymph node metastasis in T1 stage colorectal carcinomas. Dis Colon Rectum. 2003;46(12):1626-32.
13. Egashira Y, Yoshida T, Hirata I, et al. Analysis of pathological risk factors for lymph node metastasis of submucosal invasive colon cancer. Mod Pathol. 2004;17(5):503-11.
14. Watanabe T, Itabashi M, Shimada Y, et al. Japanese Society for Cancer of the Colon and Rectum (JSCCR) guidelines 2010 for the treatment of colorectal cancer. Int J Clin Oncol. 2012;17(1):1-29.
15. Smith KJ, Jones PF, Burke DA, et al. Lymphatic vessel distribution in the mucosa and submucosa and potential implications for T1 colorectal tumors. Dis Colon Rectum. 2011;54(1):35-40.
16. Roberts N, Magee D, Song Y, et al. Toward routine use of 3D histopathology as a research tool. Am J Pathol. 2012;180(5):1835-42.
17. Abdalla SA, Behzad F, Bsharah S, et al. Prognostic relevance of microvessel density in colorectal tumours. Oncol Rep. 1999;6(4):839-42.
18. Bossi P, Viale G, Lee AK, et al. Angiogenesis in colorectal tumors: microvessel quantitation in adenomas and carcinomas with clinicopathological correlations. Cancer Res. 1995;55(21):5049-53.
19. Cianchi F, Palomba A, Messerini L, et al. Tumor angiogenesis in lymph node-negative rectal cancer: correlation with clinicopathological parameters and prognosis. Ann Surg Oncol. 2002;9(1):20-6.
20. Engel CJ, Bennett ST, Chambers AF, et al. Tumor angiogenesis predicts recurrence in invasive colorectal cancer when controlled for Dukes staging. Am J Surg Pathol. 1996;20(10):1260-5.
21. Vermeulen PB, Van den Eynden GG, Huget P, et al. Prospective study of intratumoral microvessel density, p53 expression and survival in colorectal cancer. Br J Cancer. 1999;79(2):316-22.
22. Vermeulen PB, Verhoeven D, Fierens H, et al. Microvessel quantification in primary colorectal carcinoma: an immunohistochemical study. Br J Cancer. 1995;71(2):340-3.
23. Yasuda K, Inomata M, Shiromizu A, et al. Risk factors for occult lymph node metastasis of colorectal cancer invading the submucosa and indications for endoscopic mucosal resection. Dis Colon Rectum. 2007;50(9):1370-6.
24. Prall F, Nizze H, Barten M. Tumour budding as prognostic factor in stage I/II colorectal carcinoma. Histopathology. 2005;47(1):17-24.
25. Griffiths JD. Extramural and intramural blood-supply of colon. Br Med J. 1961;1(5222):323-6.
26. Standring S, editor. Gray's Anatomy, The Anatomical Basis of Clinical Practice 40th. ed: Churchill Livingstone Elsevier; 2008.

TABLE 1

Clinicopathological factors	StudyParticipants (IQR) n=26
Sex	
Male	11
Female	15
Median age at operation, years (range)	68 (62.5- 75.6)
Location of sample*	
Colon	16
Rectum	14
Embryological location of sample*	
Mid gut	10
Hind gut	20
Preoperative treatment	
Chemo-radiotherapy	4
Chemotherapy	2
Radiotherapy	2
None	18
Nodal status of tumour	
Positive	15
Negative	11
Tumour Stage	
pT1- pT2	7
pT3-pT4	19
Distant metastasis	
Present	0
Not Present	26

Table 1

Demographic information of participants included. Data were obtained from pathology reports and patient records following pathological examination of the resection specimens post-surgery. *Thirty tissue samples were collected from 26 patients, 4 of whom had 2 samples analysed from different locations within the large bowel.

Table 2A: Median values (IQR)	Number, per 0.2 μm^2 (IQR)	Circumference, µm (IQR)	Area, μm^2 (IQR)	Diameter, µm (IQR)
mucosa	11.79 (9.06-17.17)	61.9 (53.9-72.2)	247 (162-373)	7.88 (6.77-10.30)
sm1	11.44 (9.20-14.81)	99.3 (91.2-119.2)	1064 (819-1833)	16.01 (13.59-18.88)
sm2	6.92 (4.99-9.52)	134.4 (85.2-156.1)	2086 (1007-4784)	18.90 (15.69-24.32)
sm3	7.83 (5.57-9.56)	83.1 (69.5-106.4)	804 (411-1146)	13.19 (10.11-14.63)

Table 2B: Significance p values		Number	Circumference	Area	Diameter
Kruskal-Wallis Test	All (mucosa v sm1 v sm2 v sm3)	0.001	0.001	0.001	0.001
Mann-Whitney U Test	mucosa v sm1	0.492	0.001	0.001	0.001
	mucosa v sm2	0.001	0.001	0.001	0.001
	mucosa v sm3	0.001	0.001	0.001	0.001
	sm1 v sm2	0.001	0.117	0.005	0.033
	sm1 v sm3	0.001	0.030	0.032	0.002
	sm2 v sm3	0.492	p=0.001	0.001	0.001

Table 2

2A: The median vessel characteristics (and IQR values) for each layer obtained from the 12 columns from each of the 30 samples. **2B:** Statistical significance values obtained when comparing different layers using Kruskal-Wallis and Mann-Whitney U tests. Deep group includes Sm2 and Sm3 layers and is compared to Sm1 layer.

Figure Legends

Figure 1

1A: Image showing CD31 immunostaining of blood vessels and corpuscles contained within blood vessels (x200 magnification). **1B:** Image showing D2-40 immunostaining of lymphatic vessels (x400 magnification). **1C:** Imaging of double immunostained lymphatic (brown – thin arrow, D2-40) and blood (pink/red – thick arrow, CD31) vessels and ~~there~~ their close association(x400 magnification).

Figure 2

Placement of boxes (each 0.2 mm^2) for vascular analysis in normal colon**.**

2A: Illustration demonstrating the distribution of boxes throughout the layers of the bowel wall. The mucosal box (A-E) is applied randomly along the length of the section. Three boxes were then placed below this in the submucosa forming columns; each submucosal box spans one third of the depth of the submucosa (Sm1, Sm2 and Sm3).

2**B:** Image of CD31 immunostained and annotated slide, using the method as outlined above (x 400 magnification).

Figure 3

Image of the 3D model of lymphovascular structures in relation to bowel structures. Red represents blood vessels, yellow represents lymphatic vessels, purple represents mucosal lymphoid follicles, dark blue represents *musclularis propria* and bright blue represents *muscularis mucosa* . **3A:** ~~through bowel wall;~~ longitudinal segment through bowel wall; bowel lumen situated superiorly. **3B:** ~~through bowel wall; transverse~~ horizontal segment through bowel wall; bowel lumen situated superiorly. **3C:** ~~from bowel~~intra-luminal view of mucosal surface ~~lumen~~. 3D: muscularis mucosa with blood

and lymphatic vessels only, (lymphoid follicles removed) demonstrating the confinement of lymphatic vessels to the base of the mucosa.

Figure 4

The relative change in the rate of lymph node metastasis compared to the rate of change in accumulated circumference and area between submucosal layers. The relative change between submucosal layers has been calculated based on the risk of LNM as determined by Kikuchi *et al.* (sm1; 2%, sm2; 8%, sm3; 23%). The increase in the accumulated circumference or area (calculated by multiplying the median number of vessels in each layer by circumference or area, and accrued with depth) is shown to increase at a different rate to the risk of LNM.

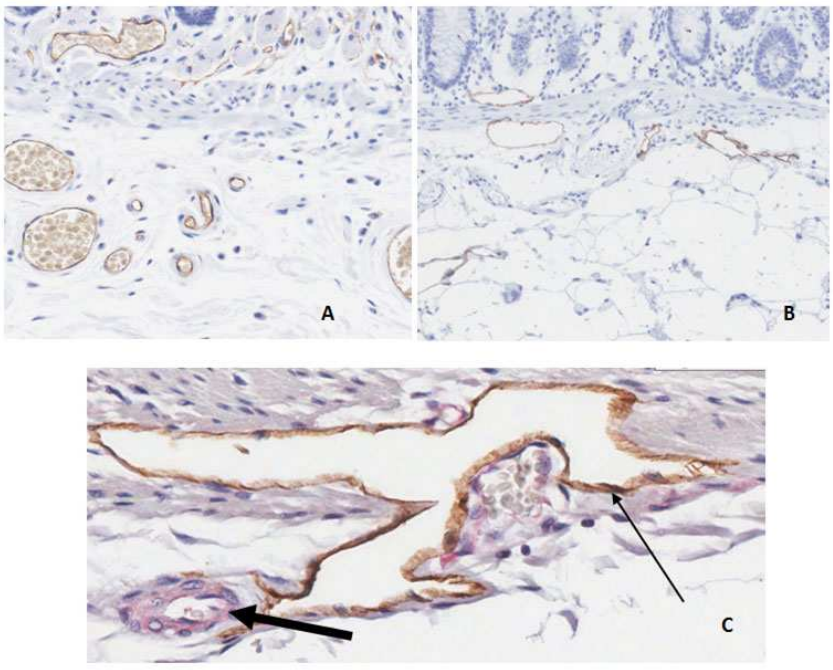

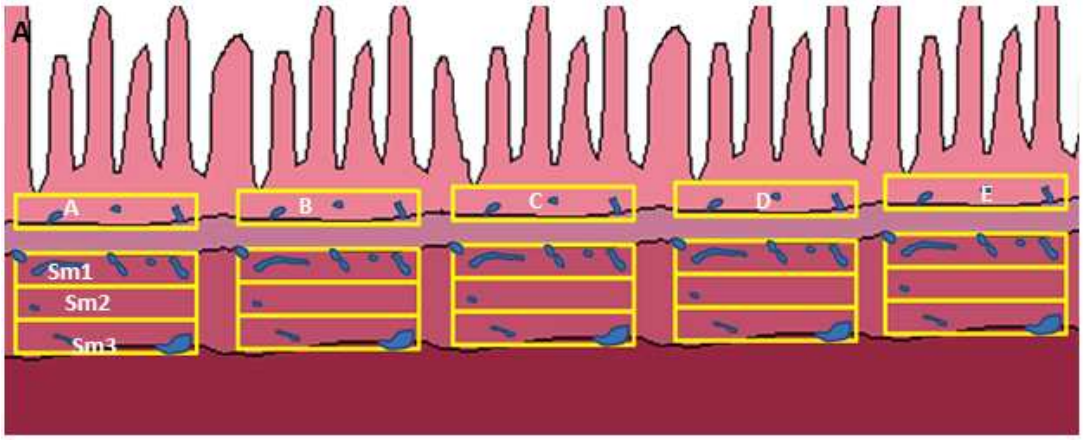

B